

Towards Wearability in Fingertip Haptics: A 3-DoF Wearable Device for Cutaneous Force Feedback

Domenico Prattichizzo, *Member, IEEE*, Francesco Chinello, Claudio Pacchierotti, *Student Member, IEEE*, and Monica Malvezzi, *Member, IEEE*

Abstract—Wearability will significantly increase the use of haptics in everyday life, as has already happened for audio and video technologies. The literature on wearable haptics is mainly focused on vibrotactile stimulation, and only recently, wearable devices conveying richer stimuli, like force vectors, have been proposed. This paper introduces design guidelines for wearable haptics and presents a novel 3-DoF wearable haptic interface able to apply force vectors directly to the fingertip. It consists of two platforms: a static one, placed on the back of the finger, and a mobile one, responsible for applying forces at the finger pad. The structure of the device resembles that of parallel robots, where the fingertip is placed in between the static and the moving platforms. This work presents the design of the wearable display, along with the quasi-static modeling of the relationship between the applied forces and the platform's orientation and displacement. The device can exert up to 1.5 N, with a maximum platform inclination of 30 degree. To validate the device and verify its effectiveness, a curvature discrimination experiment was carried out: employing the wearable device together with a popular haptic interface improved the performance with respect of employing the haptic interface alone.

Index Terms—Haptic interfaces, force feedback, wearable computers, portable computers

1 INTRODUCTION

WEARABILITY will open many opportunities to exploit haptics in everyday life and will improve the way humans interact with each other and the surrounding environment. Think, for instance, about the possibility of taking your haptic interface wherever you go, use it to get in touch with your family while you are abroad [1], touch the brand new sofa you are about to buy, or telemanipulate a remote robotic system [2]. Wearable haptic systems shall be comfortable to be carried around and well integrated into people habits, with the aim of providing valuable services to the users. Moreover, they shall be intrinsically integrated with the human body and fit it without constraining its motion, or requiring additional voluntary actions to be held.

Many haptic devices have been studied and designed to be portable or wearable, and there are three main approaches used to generate haptic feedback in wearable devices: 1) systems generating vibrations, 2) pin-arrays locally deforming the skin to simulate a given shape, and 3) mechanisms applying three-dimensional vector forces at one or more contact points.

- D. Prattichizzo and C. Pacchierotti are with the Department of Information Engineering and Mathematics, University of Siena, via Roma 56, Siena 53100, Italy, and with the Department of Advanced Robotics, Istituto Italiano di Tecnologia, via Morego 30, 16163 Genova, Italy.
- F. Chinello and M. Malvezzi are with the Department of Information Engineering and Mathematics, via Roma 56, Siena 53100, Italy.

Manuscript received 6 Oct. 2012; revised 4 Mar. 2013; accepted 3 Sept. 2013; published online 16 Oct. 2013.

Recommended for acceptance by E. Colgate.

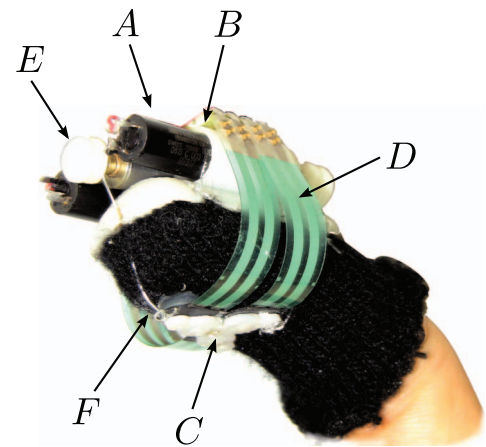
For information on obtaining reprints of this article, please send e-mail to: toh@computer.org, and reference IEEECS Log Number TH-2012-10-0081. Digital Object Identifier no. 10.1109/ToH.2013.53.

Vibrotactile feedback became popular in the 1990s with the advent of mobile phones and the innovative DualShock game controller produced by Sony. Nowadays, one of the most popular portable device providing vibrations is the game interface Wii Remote motion controller (Nintendo Co. Ltd., Japan). The form factor and weight of this device facilitate its portability. However, it can only provide very simple vibrating patterns, limiting its possibility of properly simulating any rich contact interaction with virtual or remote objects. Traylor and Tan [3] presented a vibrating wearable device able to impart directional information on the user's back. The tactile display consisted of a single tactor strapped to the volar side of the user's forearm. An accelerometer was placed on top of the tactor to record its displacement during signal delivery. The authors of [4] developed a 5-DoF arm suit able to guide the motion of the wearer by providing solely vibrotactile feedback. The suit was composed of eight vibrotactile actuators distributed throughout the right arm, whose frequency and amplitude were independently controlled. Kim et al. [5] developed a vibrotactile display to provide safety information to drivers. The device was placed on top of the foot and was composed of a 5×5 array of vibrating motors. More recently, a vibrating haptic bracelet has been used in [6] for human-robot interaction in leader-follower formation tasks. The bracelet consisted of three vibrating motors providing the user with relevant information about robot formation. For all these wearable devices, the stimuli applied to the user consisted of sinusoidal signals varying in their intensity and frequency. Although these haptic devices can be considered wearable, their force feedback is limited to vibrations, thus limiting their possibility of simulating richer force patterns.

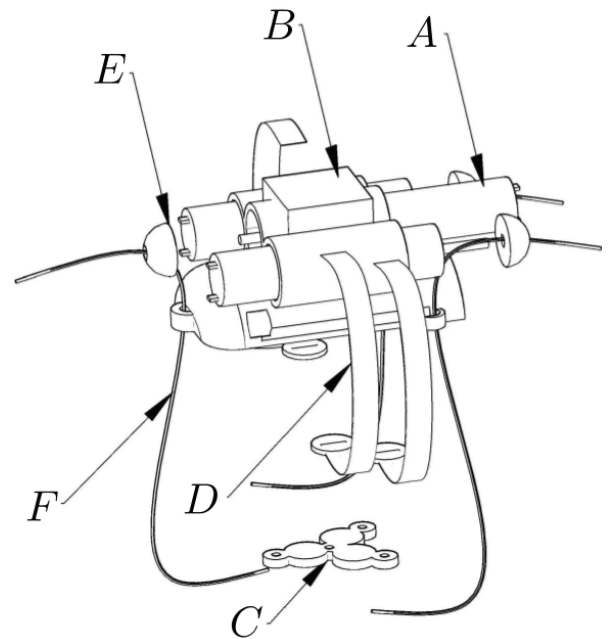
The second approach for providing haptic force feedback with wearable devices deals with dynamic pin arrays. Yang et al. [7] developed a cutaneous display composed of a 6×5 pin-array, actuated by piezoelectric bimorph actuators. It was able to display planar and Braille cell patterns to the fingertips. Pin-arrays are also employed in [8], where the authors used a solenoid, a permanent magnet, and an elastic spring to develop a miniature cutaneous module. Although this kind of display is very flexible and effective, it usually employs a large number of actuators, which compromises the overall wearability and portability of the system. For this reason, Sarakoglou et al. [9] proposed a compact 4×4 tactors array, remotely actuated through a flexible tendon transmission. Their implementation achieved a compact design, but it still required an external drive unit for the actuation system, thus compromising portability.

The third approach to wearable haptics consists of applying three-dimensional force vectors at given points on the human body. These devices are the closest, in terms of interaction modality, to grounded haptic interfaces, since both are able to apply forces at one contact point. Their distinguishing characteristic is that they need one motor for each component of the force to be independently rendered, and, for this reason, it is quite difficult to make them wearable and portable.

Glove-type haptic displays, such as the CyberGrasp (CyberGlove Systems LLC, San Jose, CA), are the most popular devices of this type and they can provide force vectors to all five fingers of the hand simultaneously. However, the mechanics of these displays is usually rather complex, thus compromising their wearability and portability. Wearability of this kind of device has been dramatically improved in [10], where Minamizawa et al. presented a wearable and portable ungrounded haptic display able to apply cutaneous forces to simulate weight sensations of virtual objects. The approach was based on the novel insight that cutaneous sensations make a reliable weight illusion, even when the kinesthetic information is absent. The device consisted of two motors and a belt able to deform the fingertip. When motors spun in opposite directions, the belt applied a force perpendicular to user's fingertip, while if motors spun in the same direction, the belt applied a shear force to the skin. That device was also used in [11] to examine the role of cutaneous and kinesthetic feedback in weight sensations, and in [1] for experiences of remote tactile interaction. However, the device proposed by Minamizawa et al. was only able to render forces in two directions: the force control was open loop and it was not very accurate. The main issue was that its control accuracy largely depended on the viscoelastic parameters of the fingerpad, which change with different subjects [12]. More recently, Solazzi et al. [13] developed an effective 3-DoF wearable cutaneous display, but the portability and wearability of the device was limited by its mechanical structure. The motors were placed on the forearm and two cables for each actuated finger were necessary to transmit the motor torque. Provancher et al. [14] proposed a fingertip device with two degrees of freedom. The device used two RC servo motors and a compliant flexure stage to create planar motion. The servos could operate simultaneously, allowing motion along any path in a plane. Another interesting device has been



(a) Prototype worn on the index finger.



(b) Computer-aided design (CAD) sketch.

Fig. 1. The 3-DoF wearable haptic display. The device is composed of two platforms: one static (B), which supports three motors (A), and one mobile (C), which is in charge of applying the requested force to the finger pad. The actuators tilt the mobile platform by means of three cables (F) and pulleys (E). Moreover, three force sensors (D) make possible to register the force applied to the fingertip.

developed in [15], where the authors presented a fingertip device which provided the user with the cutaneous sensation of making and breaking contact with virtual surfaces. However, this display had no actuation and relied on the haptic feedback provided by the haptic device it was attached to.

1.1 Contribution

This paper introduces design guidelines for the development of wearable haptic devices and presents a novel 3-DoF wearable display able to apply cutaneous forces to the finger pad. A prototype of the device, worn on the index fingertip, is shown in Fig. 1a.

This work has been inspired by the gravity grabber interface, presented in [10], which generates forces by

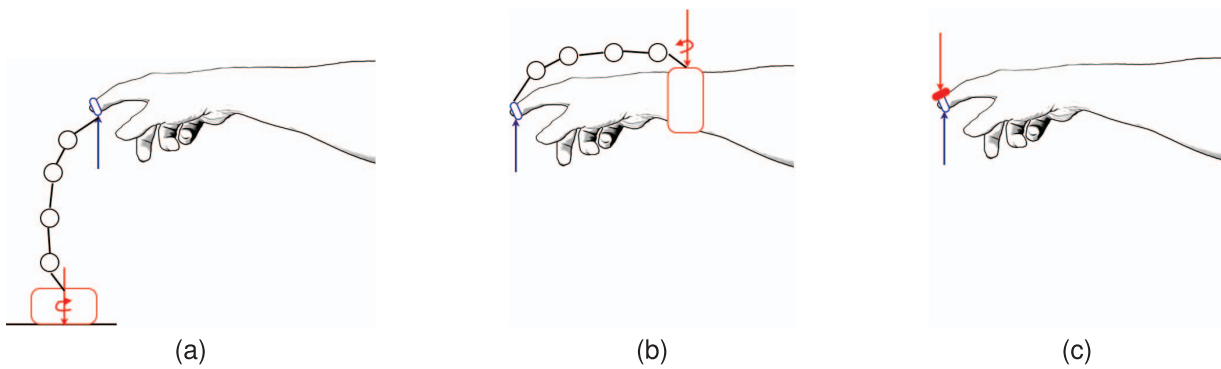


Fig. 2. From grounded to wearable haptics. Grounded haptic devices (a), exoskeletons (b), and wearable interfaces (c). In (c), the wearability is improved at the cost of losing most of the kinesthetic component of the interaction.

means of a single cable and two actuators. The device proposed here greatly differs from it, since it is designed as a 3-DoF parallel mechanism [16]: the static part is fixed on the back of the finger, and the mobile platform, or end effector, is in contact with the finger pulp. The device applies normal and tangential shear forces to the fingertip by controlling the tension of three cables by means of three actuators. Moreover, to avoid calibration problems, the cutaneous device integrates force sensors between the finger and the mobile platform. A closed-loop control of force is thus possible, and increases force control accuracy. The wearability of cutaneous devices, like the one proposed in this paper and the gravity grabber, is gained at the expense of kinesthetic feedback, which is missing.

The 3-DoF wearable interface has been preliminarily presented in [17]. In this paper, we extend the discussion on wearability, the analysis of the model, and control of the device, its performance evaluation, and we introduce design guidelines for the development of wearable haptic devices.

The paper is organized as follows: Section 2 presents guidelines for the development of a wearable haptic interface, along with the structure and working principles of the proposed device. Section 3 discusses the device closed-loop control. An experiment, carried out to validate the device and verify its effectiveness in the reproduction of cutaneous sensations, is presented and discussed in Section 4. Finally, Section 6 gives concluding remarks and perspectives of the work.

2 WEARABLE FINGERTIP HAPTIC DEVICE

2.1 Design Guidelines

Most of the well-known haptic devices for single-point contact interaction, such as the Omega (Force Dimension, Nyon, Switzerland) or the Phantom (Sensable group, Geomagic, 3D Systems, Rock Hill, SC), provide kinesthetic feedback to the user [18]. However, these devices also provide cutaneous feedback to the fingertips if we assume that the interaction with the virtual environment is mediated by a stylus, a ball, or any other tool mounted on the haptic interface [19], [20]. These devices are known as grounded interfaces (see Fig. 2a) and, although they are very accurate and able to provide a wide range of forces, their form factor is very far from being portable and wearable.

Wearability in haptics is gained with the body-grounded design of exoskeletons, where the robotic system is worn by the human operator [21], [22]. However, the main drawback of body-grounded haptics is that two forces are applied to the user: the contact force simulating the interaction and an *undesired* reaction force, which counterbalances the first one (see Fig. 2b). A good design principle is to distribute this reaction force onto a large contact surface, thus making it less perceivable than the one employed to simulate the contact interaction [22].

To improve wearability, we need to go beyond exoskeletons, reducing the mechanical complexity of the device. This may be obtained by moving the body-grounded base as close as possible to the point of application of the force, as sketched in Fig. 2c, where the base has been moved from the forearm to the nail. Removing the exoskeleton makes the devices extremely wearable, but presents the drawback of reducing the haptic interaction to cutaneous stimuli only, since the kinesthetic component cannot be provided anymore [20]. However, reducing haptic feedback to the cutaneous component only should not be seen as a problem, but as an opportunity to design more wearable devices. Indeed, recent studies assert that cutaneous stimuli are fundamental in recognizing shapes [23], in curvature discrimination tasks [17], [24], [25] and to improve the illusion of presence in virtual and remote environments [1], [19], [26], [27], [20]. We, therefore, expect cutaneous feedback to provide the user with a reliable illusion of telepresence, as the cutaneous force feedback is perceived where it is expected (i.e., the fingertip) and provides the operator with a direct and colocated perception of the contact force, even though kinesthesia is missing.

2.2 Fingernail-Grounded Device

The proposed wearable fingertip device, which implements the design guidelines discussed above, is sketched in Fig. 1b, while a prototype worn on the index fingertip is shown in Fig. 1a. The device is able to provide cutaneous forces only and it is composed of two main parts: the first one (named B in Fig. 1) is grounded to the fingernail and supports three small DC motors (named A in Fig. 1), while the active part is composed of a mobile contact platform placed on the fingertip's volar surface (C). These two parts are connected by three wires (F) whose lengths and strains are controlled by the motors through three pulleys (E). The actuators we

used for the prototype are three 0615S motors (Dr. Fritz Faulhaber GmbH & Co. KG, Schönaich, DE), with planetary gear-heads having 16:1 reduction ratio. The maximum stall torque of the motors, after the gearbox, is 3.52 mNm. The mobile platform has a Y shape and allows simulation of contact interaction with slanted surfaces. The desired contact surface orientation is achieved by modifying the forces applied to the platform vertices. Three 400 FSR (Interlink Electronics, Camarillo, CA) piezoresistive force sensors (D in Fig. 1) are placed near to the platform vertices, in contact with the finger, to measure the force applied to the fingertip. They have a diameter of 5 mm and a thickness of 0.3 mm. The small size makes them very transparent to the user and easily integrated with the device. These sensors are also useful for the initial calibration of the cutaneous system, since different fingertips require different initial positions of the mobile platform.

The contact force applied by the device to the finger pad is balanced by the structure of the device, which exerts a counterbalancing force on the back of the finger and the nail. However, the force applied by the device is still mainly perceived on the finger pad, rather than on its back, since the static structure has a larger contact surface with respect to the active mobile platform (see Section 4.2 and [20]). The local pressure is, thus, much lower. Moreover, the back of the finger, especially the nail, is less sensitive to tactile stimuli than the finger pulp. The nail also prevents problems regarding the compliance of the tissue, which may otherwise require a higher displacement to produce perceptible forces [28].

The mobile platform and the mechanical support for the actuators are made with a special type of acrylonitrile butadiene styrene, called ABSPlus (Stratasys, Eden Prairie, MN). The device can be also embedded in a finger glove, to fasten it tightly to the user's finger and make it easier to wear (see Fig. 1a). The total weight of the prototype device, including sensors, actuators, wires, and the mechanical support is about 30 g. It is worth noting that the device has no direct measurement of motor/cable position and that it is powered by two external 3.7 V 2 Ah batteries, which can be placed on the user's wrist. A cable then connects the device to its batteries. It is also worth highlighting that these cables, one for each cutaneous device being worn, could compromise the overall wearability and portability of the system. For this reason, in the next future, we are going to develop a glove embedding the finger-worn devices, the batteries, and the cables. The evaluation of the perceived wearability of the system will be discussed in Section 4.

2.3 Force and Fingertip Deformation

The device actuators, through the wires, move the platform on the fingertip. Let us indicate with $\xi = [p_x \ p_y \ p_z \ \alpha \ \beta \ \gamma]^T$ the displacement of the platform from an initial reference equilibrium condition in which the fingertip is not stimulated. Since the finger pulp is compliant, the displacement of the platform produces a deformation of the fingertip that leads to a contact stress distribution. In a quasi-static condition, the stress distribution on the fingertip is balanced by the wrench w_p applied by the platform [29]. A relationship between platform configuration ξ and wrench w_p can be, thus, assessed.

Toward this objective, let us recall some of the mathematical and numerical models for the human fingertip which have been proposed in the literature. In [30], for example, Srinivasan and Danekkar described a 2D continuum fingertip model, in which the finger was approximated by a homogeneous, isotropic, and incompressible elastic material. In [29], Serina et al. proposed a model incorporating both inhomogeneity and geometry of the fingertip. The underformed fingertip was modeled as an axial symmetric ellipsoidal elastic membrane, filled with an incompressible fluid with an internal pressure. The model was 2D and an external load was applied to the finger through a flat surface. The model predicted a pulp force/displacement relationship which could be represented as a nonlinear hardening spring, i.e., whose stiffness increases with the applied load. Most of the displacement was reached with a load of 1 N, which corresponded to a displacement of about 2 mm. In [31], Wu et al. presented a 2D finite-element model of the fingertip: the skin was modeled as a hyperelastic and viscoelastic membrane, and the subcutaneous layer was considered a biphasic material. Nakazawa et al. [32] studied the force/deformation behavior of the fingertips in the lateral, or shearing, direction. The impedance characteristics of the fingertip in the direction tangential to the tip surface were experimentally measured, and a simplified Kelvin model was adopted to describe the relationship between applied shear force and finger deformation. The experiments showed that the fingertips have different stiffness properties in the shearing direction, for example, the thumb was found stiffer than any other finger. Moreover, the shearing stiffness depended on the force direction: fingers were found stiffer in the pointing direction than in the lateral one. Actually, the stress/strain behavior of the fingertip under shearing forces is nonlinear: Wang and Hayward [33] experimentally quantified the anisotropic and hysteretic behavior of fingertip deformation under the application of shear forces.

In this paper, we consider a simplified model of the fingertip, i.e., a linear relationship between resultant wrench and platform displacement. In other terms, we assume that the platform configuration ξ is proportional to the wrench $w_p = [f_p^T \ m_p^T]^T \in \mathbb{R}^6$ applied to the mobile platform

$$\xi = K^{-1} w_p, \quad (1)$$

where $K \in \mathbb{R}^{6 \times 6}$ is the fingertip stiffness matrix. An isotropic elastic behavior is considered here for the sake of simplicity, so that the stiffness value is the same for all the elements of the matrix diagonal:

$$K = \begin{bmatrix} k_t I & 0 \\ 0 & k_r I \end{bmatrix}$$

with $k_t = 0.5$ N/m and $k_r = 0.5$ Nm/rad [34].

2.4 Three-DoF Actuated Platform

The mobile platform is actuated by three cables whose lengths and strengths are controlled by three motors. The main geometrical parameters of the device are shown in Fig. 3. B_1 , B_2 , and B_3 are the points, on the platform, where the cables, linking the mobile patch to the three actuators, pass. The reference frame $s_1 = \langle x, y, z \rangle$ is fixed to the mobile platform and its origin P_1 is placed at the geometric center of the triangle defined by points B_i . Let A_1 , A_2 , and A_3 be the vertices of the fixed platform and $s_0 = \langle X, Y, Z \rangle$ a reference

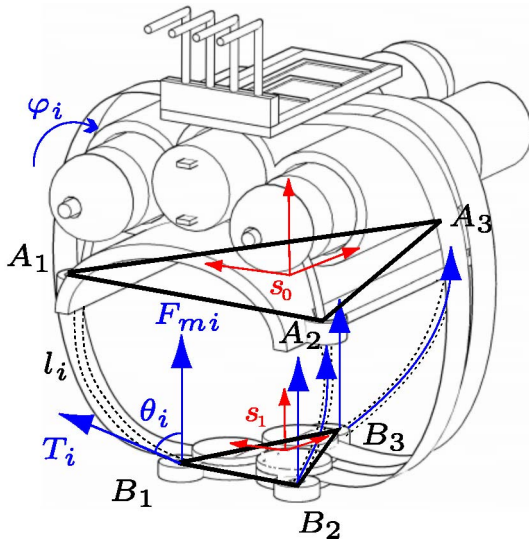


Fig. 3. The 3-DoF device kinematic scheme. Force sensors on the mobile platform measure the normal component of the force applied to the fingertip.

frame on that platform, whose origin is located at P_0 . A_i and B_i coordinates are summarized in Table 1, expressed with respect to s_0 and s_1 reference frames, respectively.

Transformation from frame s_1 to the fixed frame s_0 is described by a vector $p = P_1 - P_0$ and a 3×3 rotation matrix R_1^0 , defined as a function of the yaw (γ), pitch (β), and roll (α) angles.

2.5 Statics

Let $T = [T_1 \ T_2 \ T_3]^T$ be the vector of force magnitudes applied by the wires to the platform. These forces are balanced by the wrench due to the deformation of the fingertip. The following equilibrium condition, thus, holds:

$$w_p = J^T T, \quad (2)$$

where J is the Jacobian matrix of the structure, defined as

$$J = \begin{bmatrix} s_1^T & (b_1 \times s_1)^T \\ s_2^T & (b_2 \times s_2)^T \\ s_3^T & (b_3 \times s_3)^T \end{bmatrix}, \quad (3)$$

where s_i represent the unit vectors describing the direction of the cable force and b_i the coordinates of points B_i , expressed with respect to frame s_0 [16].

We observe that a generic wrench w_p can be reproduced by the platform if it belongs to the \mathbb{R}^6 subspace, whose basis is defined by the columns of J^T . In this case, the corresponding cable tensions can be evaluated as

$$T = (J^T)^\# w_p, \quad (4)$$

where $(J^T)^\#$ is the pseudoinverse of the Jacobian transpose. If we neglect the friction between the cable and the finger skin, cable strength can be assumed constant over the cable, and then, the relationship between actuator torques and cable strengths is simply given by

$$Q_i = T_i r_i, \quad (5)$$

TABLE 1

Point Coordinates on the Two Platforms: (a) Points A_i on the Fixed Platform with Respect to s_0 [mm], (b) Points B_i on the Mobile Platform with Respect to s_1 [mm]

	x	y	z		x	y	z
A_1	-8	-13	0	B_1	-9	-6	0
A_2	8	-13	0	B_2	9	-6	0
A_3	0	13	0	B_3	0	6	0

(a)

(b)

where $r_i, i = 1, 2, 3$ represents the radius of the i th actuator pulley.

On the other hand, if the friction between the wires and the lateral part of the fingertip cannot be neglected, the relationship between cable strengths at the motor side, $T_{a,i}$, and those at the mobile side, T_i , can be approximated as

$$T_{a,i} = T_i e^{f\alpha_i}, \quad (6)$$

where f represents the friction coefficient between the wire and the skin, and $\alpha_i, i = 1, 2, 3$ is the adhesion angle with the fingertip, depending on the fingertip curvature radius and on the length of the contact arc between the wire and the fingertip surface.

Let us also recall that the mobile platform includes three force sensors, as shown in Figs. 1 and 3. Since their sensing areas are placed next to the platform vertices, we can assume that the measured forces $F_{m,i}, i = 1, 2, 3$ are applied in B_1, B_2 , and B_3 , respectively. This assumption is partially validated by preliminary experimental tests which showed that sensors' measures are well decoupled: by actuating one motor at a time, we registered significant force variation on the corresponding sensor only, while in the other two, the force sensed was negligible. We can then assume that force sensors measure the component of each cable force normal to the platform, i.e.,

$$F_{m,i} = T_i s_i \cdot k = T_i \cos \theta_i, \quad (7)$$

where T_i is the cable tension, k the unit vector parallel to direction z , and θ_i the angle between the z axis and the s_i vector (see Fig. 3).

It is worth noting that $F_{m,i}$ depends both on the amplitude of cable tension T_i and on the configuration of the mobile platform. In particular, angle θ_i can be evaluated as a function of the relative configuration between the fixed and the mobile platform, and according to the fingertip geometry and curvature.

2.6 Kinematics

The distance between platforms' vertices $d_i = B_i - A_i$, for a given displacement p and an angular configuration, can be evaluated as

$$c_i = \|d_i\| = \sqrt{a_i^2 + b_i^2 - 2a_i b_i \cos \theta_i} \quad i = 1, 2, 3, \quad (8)$$

where c_i is the distance between the i th vertices, and $a_i, i = 1, 2, 3$, represent the coordinates of points A_i , expressed with respect to frame s_0 . From the distance between the

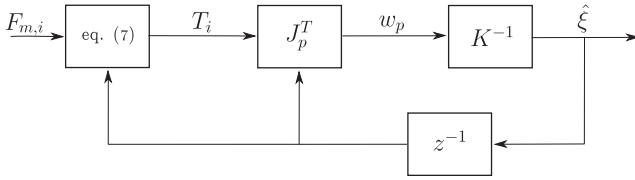


Fig. 4. Estimation of platform position $\hat{\xi}$ and wrench \hat{w}_p .

vertices and from the finger curvature radii R_i (which can be approximately considered constant), we can evaluate the actual length of cables l_i , and, consequently, motor rotations $q_i = \varphi_i$ as

$$q_i = \frac{l_i}{r_i} = 2 \frac{R_i}{r_i} \arcsin\left(\frac{c_i}{2R_i}\right). \quad (9)$$

2.7 Wrench and Posture Estimation

From the above kinematic and static analysis, a procedure for online estimation of contact forces and platform configuration has been developed.

Let us assume platform displacement to be small with respect to the platform geometric dimensions. Assume also that the initial platform configuration $\xi(0)$ is known and that the sampling time is small, so that the variation of configuration between two consecutive integration steps is small, i.e., for a generic time step j , $\xi(j) \cong \xi(j-1)$.

The estimation algorithm is reported in the block diagram shown in Fig. 4 and summarized below.

Algorithm 1 Estimate wrench and platform orientation

for each time sample j **do**

1. read from the sensors the normal component of the contact forces $F_{m,i}(j)$, $i = 1, 2, 3$,
2. approximate cable forces \hat{T}_i as described in eq.(7),
3. estimate platform wrench $\hat{w}_p(j)$ as described in eq. (2),
4. estimate platform configuration $\hat{\xi}(j)$ by means of the compliant model defined in eq. (1),
5. solve the inverse kinematic problem of the platform and find angles $\hat{\theta}_i(j)$.

end for

3 CONTROL

The device described in the preceding sections is inherently underactuated: since it has only three motors, no more than three components of force/displacement can be controlled, independently, at the same time. For example, if we need to control the three Cartesian components of the contact force resultant, by acting on the cable strengths, we cannot, at the same time, choose the orientation of the platform. On the other hand, when controlling platform orientation, the device can rotate the platform in the X and Y (lateral and longitudinal) directions and the remaining available degree of freedom can be used to regulate contact force magnitude. In this case, the direction of the contact force cannot be controlled.

The coupling between the applied contact force and the platform position depends essentially on the fingertip

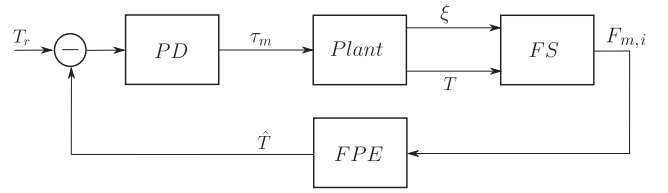


Fig. 5. Device force control. Reference force T_r is compared to the estimated one \hat{T} . The error signal serves as input for the motors PD controllers, which generate motor torque τ_m . From the force F_m , measured by the sensors (force sensors block, FS), and platform position $\hat{\xi}$, estimated at the preceding time step, force and position estimation block, detailed in Fig. 4, evaluates the wire forces \hat{T} .

compliance matrix. We present here two control strategies: the first one looks at the three Cartesian components of the force, exchanged between the platform and the fingertip, while the second one looks at the platform configuration. When one of the two control schemes is chosen, the uncontrolled parameters vary according to the whole system equilibrium. This coupling is inherently connected to the underactuated nature of the device. It is also worth noting that the device cannot control all the possible configuration and force spaces. To improve the control capabilities, the number of actuators should be increased, affecting the overall wearability of the system.

The first control scheme, shown in Fig. 5, aims at controlling cable strengths T_r . The second scheme, shown in Fig. 6 and referred to as the position-control scheme, aims at controlling platform orientation. The details of these control strategies are described in [17]. However, for the sake of completeness, the block diagrams and the main features are summarized here. In both the schemes, each motor is controlled by a closed-loop chain with a PD controller. The reference signal is transmitted via a USB-to-serial converter interface with a sampling time of $t_s = 0.01$ s.

An application in which the force-control scheme would be useful is the one described in [19], where cutaneous stimuli were employed in a 1-DoF teleoperated needle insertion task. On the other hand, position control is suitable for applications in which the shape of the virtual contact surface is more important than the contact force. An example of this type of application is described in [25], in which the authors investigated the influence of cutaneous feedback on convex surface recognition.

Both control schemes are based on force and position estimation (FPE) procedures, which depend on the finger compliance model and are referred to as FPE in the block

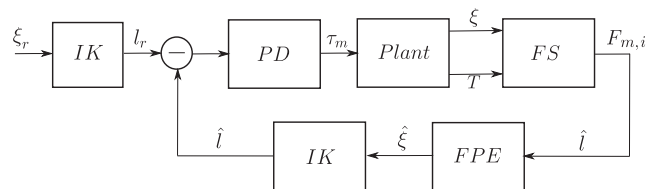
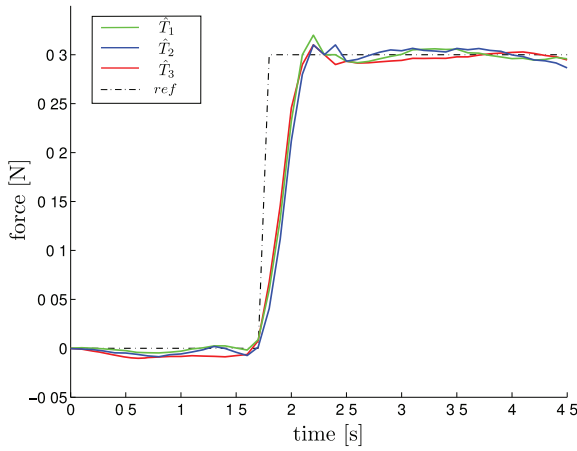
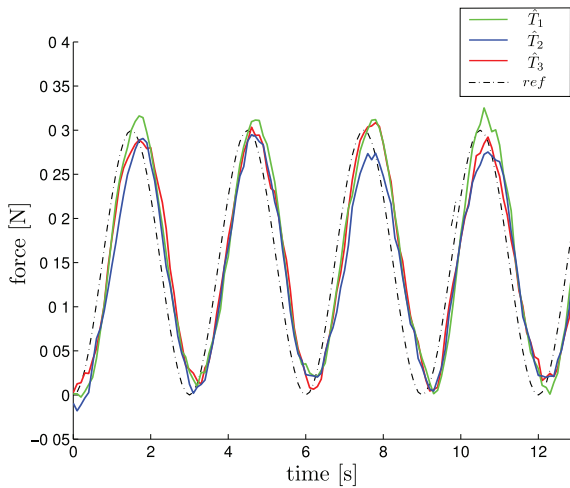


Fig. 6. Platform position control system. From reference position ξ_r , by means of the inverse kinematics procedure (IK), reference wire lengths l_r are estimated. They are then compared to the estimated ones \hat{q} , evaluated applying the IK procedure to the configuration $\hat{\xi}$, estimated in the FPE block as a function of the measured forces F_m and the position estimated at the preceding time step.



(a) Step response.



(b) Response to a variable reference force signal.

Fig. 7. Response to reference force signals. Dashed black lines represent reference force values and green, blue, and red solid lines represent the estimated wire strains \hat{T}_1 , \hat{T}_2 , and \hat{T}_3 , respectively.

diagrams in Figs. 5 and 6. In this work, we considered a linear model for the finger compliance, as described in Section 2.3. Work is in progress to investigate the sensitivity of the control performance on the finger compliance and the possibility of using different and more complex finger models.

3.1 Force Control

We characterize the force control accuracy using three measures. Fig. 7a shows the control system performance when a step signal is applied to the reference values of the cable strengths T_r . The reference force was the same for each cable: $T_{r,i} = 0.3$ N, for $i = 1, 2, 3$. In the figure, the reference value (dashed) and the estimated cable strengths \hat{T}_i are shown. Results show that the estimated forces reach the reference value with a rise time of about 0.1 s and an error in the stationary phase lower than 2 percent. The system bandwidth is about 10 Hz. Fig. 7b shows the behavior of the device when the force reference signal is sinusoidal:

$$T_{r,i} = (0.15 \sin(\pi t) + 0.15) \text{ N, for } i = 1, 2, 3.$$

We also evaluated the error between a reference force and the one registered by the force sensor. Five subjects (four males, one female) were asked to wear one cutaneous device on their index finger. The system then applied the sinusoidal reference force $T_{r,i}$ at each wire $i = 1, 2, 3$, for $t \in [0, 180]$. The RMS error was 0.021 N and its standard deviation was 0.011 N.

3.2 Position Control

To evaluate the accuracy of the position control system, an additional experimental test was performed. We fixed a three-axis accelerometer on the external surface of the mobile platform, the one not in contact with the fingertip, and we asked a user to wear this modified haptic device on his index finger. The system then simulated the contact between the finger and an arbitrarily oriented surface for $N_s = 100$ iterations. At each repetition, the system chose a random platform configuration $\xi_{r,n}$, $n = 1, \dots, 100$, with

$$\begin{aligned} p_x = p_y = 0, \quad 0 \leq p_z \leq 5 \text{ mm}, \\ 0 \leq \alpha \leq 18^\circ, \quad 0 \leq \beta \leq 18^\circ, \\ \gamma = 0. \end{aligned}$$

Then, we compared the reference configuration $\xi_{r,n}$ with the actual configuration $\xi_{a,n}$ measured by the accelerometer.

The mean error e_p , evaluated as

$$e_p = \frac{1}{N_s} \sum_{n=1}^{N_s} \sqrt{(\alpha_{r,n} - \alpha_{a,n})^2 + (\beta_{r,n} - \beta_{a,n})^2 + (\gamma_{r,n} - \gamma_{a,n})^2},$$

was 1.60 degrees and its standard deviation was 0.98 degree.

4 CURVATURE DISCRIMINATION EXPERIMENT

An experiment assessing the effectiveness of the wearable device has been carried out. Its objective was the evaluation of the difference threshold for curvature discrimination when employing kinesthetic and cutaneous force feedback together (condition H) or solely kinesthetic force feedback (condition K). A similar experiment has been carried out in [24], where the authors presented a haptic device providing both kinesthetic and cutaneous cues informative of shape geometry at the contact point. They evaluated the difference threshold for curvature discrimination when both kinesthetic and cutaneous cues were available (i.e., while using the new haptic device proposed) and when only kinesthetic cues were available (i.e., using a popular grounded kinesthetic device). After that, we also asked users about the perceived wearability, portability, and comfort in using the device.

4.1 Methods

Similarly to the work in [24], the same-different procedure of theory of signal detection (TSD) was implemented to evaluate the just noticeable difference (JND) for curvature [35], [36]. According to signal detection theory, signals are detected by humans against a noisy background. Two probability distributions describe the variations in the noise (N) and the signal-plus-noise (SN). Subjects set a criterion as a cutoff point for deciding if each observation belongs to N or to SN. On signal-plus-noise trials, positive responses are

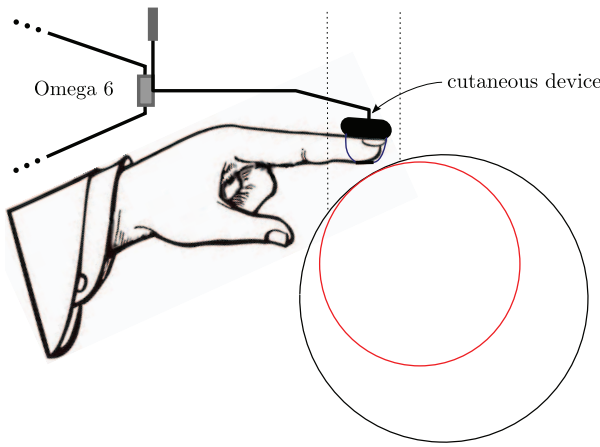


Fig. 8. Experimental setup. The exploration was carried out in a restricted workspace consisting of a vertical cylinder with a diameter of 30 mm.

correct and are termed *hits*. On noise trials, positive responses are incorrect and are termed *false alarms*. The hit rate p_h , i.e., the probability of responding *yes* on SN trials, and the false-alarm rate p_f , i.e., the probability of responding *yes* on noise trials, fully describe the performance of the task. In TSD, sensitivity can be quantified by using the hit and false-alarm rates to determine the distance between the means of the SN and N distributions, relative to their standard deviations. A sensitivity index d' is then defined as the difference between those means, divided by the standard deviation of the N distribution. The value of d' can be calculated from the false alarm and hit rates, after converting them to z scores [24], [35].

Fourteen participants (12 males, 2 females, age range 20-31, index size range 3.9-6.1 cm^1) took part in the experiment, all of whom were right-handed. Four of them had previous experience with haptic interfaces. None of the participants reported any deficiencies in their perception abilities and they were naïve as to the purpose of the study.

The experimental setup was composed of one wearable device attached to the end-effector of an Omega 6 haptic device. Subjects were blindfolded, with a support for the elbow, and were instructed to wear the device on their right index finger. According to the aforementioned TSD procedure, each trial involved exploring, in succession, a pair of virtual spheres. The exploration was carried out in a restricted workspace consisting of a vertical cylinder with a diameter of 30 mm, as shown in Fig. 8. The task consisted in judging, on each trial, if the curvature of the two surfaces was different or the same. Each participant was informed about the procedure before the beginning of the experiment, and a 10-minute familiarization period, both while using the wearable device alone and while using it attached to the Omega 6 end-effector, was given, to make the subjects acquaintance with the experimental setup.

The hit rate p_h corresponded to the percentage of correct responses given by a subject ("yes, the curvatures are different") when the two surfaces had different curvatures, while the false alarm rate p_f corresponded to the percentage

of incorrect responses ("yes, the curvatures are different") when the curvatures of the two surfaces were the same.

Two different force feedback conditions have been taken into account. In *condition H*, both the wearable device and the Omega 6 provided haptic cues to the subject. The mobile platform of the wearable device was providing cutaneous cues about the local geometry of the surface being touched, while the Omega device provided a kinesthetic force perpendicular to the given virtual surface. In *condition K*, only the Omega 6 fed back contact forces. The mobile platform of the cutaneous device was not in contact with the fingertip and its orientation was fixed. In all conditions, the Omega prevented the user from exiting the restricted exploration area (see Fig. 8).

Each subject carried out four series of trials, in which spheres with different curvature values, $\kappa_{a,*}$ and κ_b , were taken into account:

1. $\kappa_{a,1} = 3.5 \text{ m}^{-1}$ and $\kappa_b = 6 \text{ m}^{-1}$ for Series 1,
2. $\kappa_{a,2} = 4 \text{ m}^{-1}$ and $\kappa_b = 6 \text{ m}^{-1}$ for Series 2,
3. $\kappa_{a,3} = 4.5 \text{ m}^{-1}$ and $\kappa_b = 6 \text{ m}^{-1}$ for Series 3,
4. $\kappa_{a,4} = 5 \text{ m}^{-1}$ and $\kappa_b = 6 \text{ m}^{-1}$ for Series 4.

Each series consisted of 100 repetitions of the curvature discrimination task, with 50 trials for each feedback conditions H and K. The entire experiment lasted approximately 50 mins.

On each repetition of each series, two spheres with random curvature ($\kappa_{a,*}$ or κ_b) were rendered, i.e., the probability of exploring a pair of spheres with same (different) radius was 0.5. The order of presentation of the sequence of series and conditions was different for each subject, to minimize learning and fatigue effects. For each series, subjects' responses were recorded, calculating the hit and false alarm rate.

4.2 Results

False alarm and hit rate were first converted to z scores of the normal distribution [36], [35]. The sensitivity index d' was then calculated as the difference

$$d' = z_h - z_f.$$

According to the criterion commonly adopted [24], [36], the discrimination threshold can be defined as the difference between the curvatures for which $d' = 1$. The threshold was computed for each subject for each condition H and K, assuming a linear proportionality between the values of d' .

The overall JND was then computed as the mean of the values obtained for all the subjects. The collected data of each condition passed the D'Agostino-Pearson omnibus K2 normality test. Then, a parametric two-tailed paired t-test ($\alpha = 0.05$) was performed to evaluate the statistical significance of the differences between the two conditions. The average JND values were significantly lower ($p = 0.014$) for condition H than for K, with an average \pm standard deviation of 2.22 ± 0.29 and $2.56 \pm 0.36 \text{ m}^{-1}$ for conditions H and K, respectively. Time needed to complete the given tasks was recorded as well, and no statistical difference was found between the average values for the two conditions.

For the subjects enrolled in this experiment, we confirmed that, as was also discussed in [24], the combination of cutaneous and kinesthetic force feedback led to better

1. The finger size was calculated as the circumference of the fingertip at the level of the base of the nail, i.e., where the cuticle is.

TABLE 2
Users' Experience Evaluation

Questions		Mean	SD
Q1	It has been easy to wear and use the cutaneous device.	6.1	0.7
Q2	It has been easy to use the Omega 6 together with the cutaneous device.	5.0	0.7
Q3	I was feeling uncomfortable while using the Omega 6 together with cutaneous device.	2.3	0.7
Q4	I was well-isolated from external noises.	6.3	0.5
Q5	I was able to hear the sounds made by the actuators of the cutaneous device.	1.9	0.7
Q6	It was easy to feel the presence of a curved surface.	6.7	0.5
Q7	I had the feeling of performing better while receiving force feedback by the Omega 6 only.	3.4	0.8
Q8	I had the feeling of performing better while receiving force feedback by the cutaneous device.	5.2	1.0
Q9	The force given by the Omega 6 was enough to distinguish the curvature.	4.1	0.9
Q10	At the end of the experiment I felt tired.	1.4	0.5
Q11	It was easy to move my hand and fingers while wearing the cutaneous device.	6.6	0.5
Q12	I felt hampered by the cutaneous device.	1.4	0.5
Q13	I was feeling a force also on the back of the finger.	1.9	0.6
Q14	The force provided by the cutaneous device on the fingertip felt strange.	1.9	0.7
Q15	I felt the force provided by the cutaneous device only on the fingertip.	5.9	0.7

Participants rated these statements, presented in random order, using a seven-point Likert scale (1 = completely disagree, 7 = completely agree). Means and standard deviations are reported.

performance than employing kinesthetic force feedback only. These data confirmed that the display of surface orientation employing the wearable device here presented can help haptic perception of shape, and, in general, it confirmed the importance of cutaneous cues in haptics.

The discrimination threshold for curvature observed in this work is in agreement with previous results in the literature. Frisoli et al. [24] found an average JND value of 2.62 m^{-1} for kinesthetic feedback only and of 1.51 m^{-1} when providing both cutaneous and kinesthetic cues. Our cutaneous device showed worse performance with respect to the one presented in [24]; however, we believe that this is a price worth paying to gain a great improvement in the wearability and portability of the system (see also Section 2). In [37], the authors found discrimination thresholds of 3.58 and 2.6 m^{-1} for direct and virtual discrimination of spheres, respectively, for a reference curvature of 25 m^{-1} employing both kinesthetic and cutaneous force feedback. Goodwin et al. [38] measured the ability of subjects to discriminate convex spherical surfaces from a flat plane using the fingerpad alone. A curvature of 4.58 m^{-1} could be discriminated, at the 75 percent level ($d' = 1.35$), from the standard curvature of zero. The authors of [39], using real objects and a reference curvature of 33 m^{-1} , found the curvature discrimination threshold for the index finger of the preferred hand to be about 2.5 m^{-1} .

At the end of this experiment, we also asked the subjects to answer a questionnaire of 15 questions using bipolar Likert-type seven-point scales. It considered the comfort in using the proposed experimental setup (five questions), the perceived performance (five questions), and its level of wearability when detached from the Omega end-effector (five questions). An answer of 7 meant a very high wearability of the system (or comfort or perceived performance), while an answer of 1 meant a very low wearability of the system (or comfort or perceived performance). The evaluation of each question is reported in Table 2.

5 DISCUSSION

As discussed in Section 2, wearability demands for cutaneous force feedback more than kinesthesia. However, kinesthetic stimuli could be partially recovered with wearable modules able to exert partial force feedback to arm joints. The relationship between cutaneous and kinesthetic perception in haptics is, thus, an important research issue. More in general, going to wearable solutions for haptics, inherently leads to underactuated and undersensed devices, in which the cutaneous stimuli are predominant with respect to the kinesthetic one.

However, similarly to other robotic research fields, we believe that underactuation and undersensing of haptic devices represent an opportunity, and not an issue, since they allow us to simplify the actuation system, decrease the weight, lower the energy consumption, and improve the mechanical structure design, turning the haptic device into an intrinsically wearable structure. Another advantage of wearable and small-size haptic devices is that they easily allow the simultaneous stimulation of several points on the human skin. We, thus, expect that the consequent richness of information will contribute to mitigate the lack of actuation and sensing, through methods based on cognitive models and multisensory integration.

The availability of wearable haptic devices will support the investigation on complementary approaches, which interact with different parts of the human body through the sense of touch. The complexity of the wearable system will be not a priori fixed, indeed the inherently modular nature of the wearable haptic solutions will allow us to customize the system according to the given applications.

6 CONCLUSIONS AND FUTURE WORK

In this work, a novel approach for wearable fingertip haptics has been presented, along with the design of a wearable cutaneous device, as a proof of feasibility of the concepts discussed in Sections 1 and 2.

In comparison to similar existing cutaneous devices, this one has three actuated degrees of freedom and it is able to simulate a contact force with general direction at the fingertip. The device can be represented as a 3-DoF parallel mechanism in which a mobile platform is actuated modifying the strain of the three wires. The mobile platform is connected to the finger and applies a force whose direction and amplitude depend on cable strengths and on platform's position and orientation. The finger was modeled as a linear six-dimensional spring. Future development of the presented study will include the analysis of other types of fingertip model.

Two control schemes were presented: in the first one (force control), the wire strains were controlled, while in the second one (position control), the platform configuration (position and orientation) was controlled. Tests on the force control performance showed that the dynamic response of the system is stable and quite accurate. These tests also showed acceptable results in terms of response time and error, and low sensitivity with respect to finger stiffness values. To validate the device and verify its accuracy and effectiveness, we evaluated the JND in curvature discrimination. Results showed that employing the wearable device together with a popular haptic interface (task H) improved the performance with respect of employing the haptic interface alone (task K). Average JND values were significantly lower for condition H than for condition K, with an average \pm standard deviation of 2.22 ± 0.29 and $2.56 \pm 0.36 \text{ m}^{-1}$ for H and K, respectively (see Section 4.2 for details).

We strongly believe that this kind of highly wearable devices can be useful in many applications, ranging from rehabilitation to entertainment purposes, from robotic surgery to e-commerce, and will contribute in bringing haptic technologies to everyday life applications.

The device presented provides tactile stimuli only, while most of the kinesthetic feedback is missing. Possible solutions to compensate for this lack of information, while preserving the portability of the device, are currently being investigated. New experiments aiming at evaluating users' experience, while interacting with real objects and augmented scenarios will be performed in the next future. Moreover, we are planning to equip the device's actuators with position encoders to be able to provide more accurate and efficient control algorithms. Finally, we will also take into account the variability of fingertip mechanical characteristics in different users.

ACKNOWLEDGMENTS

The research leading to these results has received funding from the European Union Seventh Framework Programme FP7/2007-2013 under grant agreement no. 270460 of the project "ACTIVE—Active Constraints Technologies for Ill-defined or Volatile Environments" and under grant agreement no. 601165 of the project "WEARHAP—WEARable HAPtics for humans and robots."

REFERENCES

- [1] D. Prattichizzo, F. Chinello, C. Pacchierotti, and K. Minamizawa, "RemoTouch: A System for Remote Touch Experience," *Proc. IEEE Int'l Symp. Robots and Human Interactive Comm.*, pp. 676-679, 2010.

- [2] C. Pacchierotti, F. Chinello, M. Malvezzi, L. Meli, and D. Prattichizzo, "Two Finger Grasping Simulation with Cutaneous and Kinesthetic Force Feedback," *Haptics: Perception, Devices, Mobility, and Comm. Eurohaptics 2012*, Lecture Notes in Computer Science, pp. 373-382, 2012.
- [3] R. Traylor and H. Tan, "Development of a Wearable Haptic Display for Situation Awareness in Altered-Gravity Environment: Some Initial Findings," *Proc. 10th Symp. Haptic Interfaces for Virtual Environment and Teleoperator Systems*, pp. 159-164, 2002.
- [4] J. Lieberman and C. Breazeal, "TIKL: Development of a Wearable Vibrotactile Feedback Suit for Improved Human Motor Learning," *IEEE Trans. Robotics*, vol. 23, no. 5, pp. 919-926, Oct. 2007.
- [5] H. Kim, C. Seo, J. Lee, J. Ryu, S. Yu, and S. Lee, "Vibrotactile Display for Driving Safety Information," *Proc. IEEE Intelligent Transportation Systems Conf.*, pp. 573-577, 2006.
- [6] S. Scheggi, F. Chinello, and D. Prattichizzo, "Vibrotactile Haptic Feedback for Human-Robot Interaction in Leader-Follower Tasks," *Proc. ACM Fifth Int'l Conf. Pervasive Technologies Related to Assistive Environments (PETRA '12)*, 2012.
- [7] G. Yang, K. Kyung, M. Srinivasan, and D. Kwon, "Quantitative Tactile Display Device with Pin-Array Type Tactile Feedback and Thermal Feedback," *Proc. IEEE Int'l Conf. Robotics and Automation*, pp. 3917-3922, 2006.
- [8] T. Yang, S. Kim, C. Kim, D. Kwon, and W. Book, "Development of a Miniature Pin-Array Tactile Module Using Elastic and Electromagnetic Force for Mobile Devices," *Proc. EuroHaptics and Symp. Haptic Interfaces for Virtual Environment and Teleoperator Systems*, pp. 13-17, 2009.
- [9] I. Sarakoglou, N. Garcia-Hernandez, N. Tsarakakis, and D. Caldwell, "A High Performance Tactile Feedback Display and Its Integration in Teleoperation," *IEEE Trans. Haptics*, vol. 5, no. 3, pp. 252-263, July-Sept. 2012.
- [10] K. Minamizawa, S. Fukamachi, H. Kajimoto, N. Kawakami, and S. Tachi, "Gravity Grabber: Wearable Haptic Display to Present Virtual Mass Sensation," *Proc. ACM SIGGRAPH*, article 8, 2007.
- [11] K. Minamizawa, D. Prattichizzo, and S. Tachi, "Simplified Design of Haptic Display by Extending One-Point Kinesthetic Feedback to Multipoint Tactile Feedback," *Proc. IEEE Haptics Symp.*, pp. 257-260, 2010.
- [12] M.J. Adams, S.A. Johnson, P. Lefèvre, V. Lévesque, V. Hayward, T. André, and J.-L. Thonnard, "Finger Pad Friction and Its Role in Grip and Touch," *J. Royal Soc. Interface*, vol. 10, no. 80, 2013.
- [13] M. Solazzi, A. Frisoli, and M. Bergamasco, "Design of a Cutaneous Fingertip Display for Improving Haptic Exploration of Virtual Objects," *Proc. IEEE Int'l Symp. Robots and Human Interactive Comm.*, pp. 1-6, 2010.
- [14] B. Gleeson, S. Horschel, and W.R. Provancher, "Design of a Fingertip-Mounted Tactile Display with Tangential Skin Displacement Feedback," *IEEE Trans. Haptics*, vol. 3, no. 4, pp. 297-301, Oct.-Dec. 2010.
- [15] K. Kuchenbecker, D. Ferguson, M. Kutzer, M. Moses, and A. Okamura, "The Touch Thimble: Providing Fingertip Contact Feedback during Point-Force Haptic Interaction," *Proc. Symp. Haptic Interfaces for Virtual Environment and Teleoperator Systems*, pp. 239-246, 2008.
- [16] L.W. Tsai, *Robot Analysis: The Mechanics of Serial and Parallel Manipulators*. John Wiley & Sons, 1999.
- [17] F. Chinello, M. Malvezzi, C. Pacchierotti, and D. Prattichizzo, "A Three DoFs Wearable Tactile Display for Exploration and Manipulation of Virtual Objects," *Proc. IEEE Haptics Symp.*, pp. 71-76, 2012.
- [18] V. Hayward, O. Astley, M. Cruz-Hernandez, D. Grant, and G. Robles-De-La-Torre, "Haptic Interfaces and Devices," *Sensor Rev.*, vol. 24, no. 1, pp. 16-29, 2004.
- [19] D. Prattichizzo, C. Pacchierotti, and G. Rosati, "Cutaneous Force Feedback as a Sensory Subtraction Technique in Haptics," *IEEE Trans. Haptics*, vol. 5, no. 4, pp. 289-300, Oct.-Dec. 2012.
- [20] C. Pacchierotti, A. Tirmizi, and D. Prattichizzo, "Improving Transparency in Teleoperation by Means of Cutaneous Tactile Force Feedback," to be published in *ACM Trans. Applied Perceptions*, 2014.
- [21] S. Biggs and M. Srinivasan, "Haptic Interfaces," *Handbook of Virtual Environments: Design, Implementation, and Applications*, Taylor & Francis, pp. 93-116, 2002.

- [22] M. Bergamasco, B. Allotta, L. Bosio, L. Ferretti, G. Parrini, G. Prisco, F. Salsedo, and G. Sartini, "An Arm Exoskeleton System for Teleoperation and Virtual Environments Applications," *Proc. IEEE Int'l Conf. Robotics and Automation*, pp. 1449-1454, 1994.
- [23] G. Jansson and L. Monaci, "Identification of Real Objects under Conditions Similar to Those in Haptic Displays: Providing Spatially Distributed Information at the Contact Areas is More Important than Increasing the Number of Areas," *Virtual Reality*, vol. 9, no. 4, pp. 243-249, 2006.
- [24] A. Frisoli, M. Solazzi, F. Salsedo, and M. Bergamasco, "A Fingertip Haptic Display for Improving Curvature Discrimination," *Presence: Teleoperators and Virtual Environments*, vol. 17, no. 6, pp. 550-561, 2008.
- [25] M. Wijnjtes, A. Sato, V. Hayward, and A. Kappers, "Local Surface Orientation Dominates Haptic Curvature Discrimination," *IEEE Trans. Haptics*, vol. 2, no. 2, pp. 94-102, Apr.-June 2009.
- [26] M. Ottermo, M. Øvstedal, T. Lango, Ø. Stavadahl, Y. Yavuz, T. Johansen, and R. Mårvik, "The Role of Tactile Feedback in Laparoscopic Surgery," *Surgical Laparoscopy Endoscopy & Percutaneous Techniques*, vol. 16, no. 6, p. 390, 2006.
- [27] A. Okamura, "Methods for Haptic Feedback in Teleoperated Robot-Assisted Surgery," *Industrial Robot: An Int'l J.*, vol. 31, no. 6, pp. 499-508, 2004.
- [28] K. Kim and E. Colgate, "Haptic Feedback Enhances Grip Force Control of sEMG-Controlled Prosthetic Hands in Targeted Reinnervation Amputees," *IEEE Trans. Neural Systems and Rehabilitation Eng.*, vol. 20, no. 6, pp. 798-805, 2012.
- [29] E. Serina, E. Mockensturm, C. Mote Jr, and D. Rempel, "A Structural Model of the Forced Compression of the Fingertip Pulp," *J. Biomechanics*, vol. 31, no. 7, pp. 639-646, 1998.
- [30] M. Srinivasan and K. Danekkar, "An Investigation of the Mechanics of Tactile Sense Using Two Dimensional Models of the Primate Fingertip," *J. Biomechanical Eng.*, vol. 118, pp. 48-55, 1996.
- [31] J.Z. Wu, R.G. Dong, S. Rakheja, A.W. Schopper, and W.P. Smutz, "A Structural Fingertip Model for Simulating of the Biomechanics of Tactile Sensation," *Medical Eng. and Physics*, vol. 26, no. 2, pp. 165-175, 2004.
- [32] N. Nakazawa, R. Ikeura, and H. Inooka, "Characteristics of Human Fingertips in the Shearing Direction," *Biological Cybernetics*, vol. 82, pp. 207-214, 2000.
- [33] Q. Wang and V. Hayward, "In Vivo Biomechanics of the Fingertip Skin under Local Tangential Traction," *J. Biomechanics*, vol. 40, pp. 851-860, 2007.
- [34] K. Park, B. Kim, and S. Hirai, "Development of a Soft-Fingertip and Its Modeling Based on Force Distribution," *Proc. IEEE Int'l Conf. of Robotics and Automation*, vol. 3, pp. 3169-3174, 2003.
- [35] H. Stanislaw and N. Todorov, "Calculation of Signal Detection Theory Measures," *Behavior Research Methods*, vol. 31, no. 1, pp. 137-149, 1999.
- [36] G. Gescheider, *Psychophysics: The Fundamentals*. Lawrence Erlbaum, 1997.
- [37] W. Provancher, M. Cutkosky, K. Kuchenbecker, and G. Niemeyer, "Contact Location Display for Haptic Perception of Curvature and Object Motion," *Int'l J. Robotics Research*, vol. 24, no. 9, pp. 691-702, 2005.
- [38] A. Goodwin, K. John, and A. Marcegaglia, "Tactile Discrimination of Curvature by Humans Using Only Cutaneous Information from the Fingertips," *Experimental Brain Research*, vol. 86, no. 3, pp. 663-672, 1991.
- [39] B. van der Horst and A. Kappers, "Curvature Discrimination in Various Finger Conditions," *Experimental Brain Research*, vol. 177, no. 3, pp. 304-311, 2007.



Domenico Prattichizzo (S'93-M'95) received the MS degree in electronics engineering and the PhD degree in robotics and automation from the University of Pisa, in 1991 and 1995, respectively. Since 2002, he has been an associate professor of robotics at the University of Siena and a scientific consultant at Istituto Italiano di Tecnologia, Genova, Italy, since 2009. He was a visiting scientist at the MIT AI Lab in 1994. He is a coauthor of the Grasping chapter of *Handbook of Robotics*, Springer, 2008, awarded with two PROSE Awards presented by the American Association of Publishers. Since 2007, he has been an associate editor-in-chief of the *IEEE Transactions on Haptics*. From 2003 to 2007, he was an associate editor of the *IEEE Transactions on Robotics* and *IEEE Transactions on Control Systems Technologies*. He was a vice-chair of special issues for the IEEE Technical Committee on Haptics (2006-2010) and a chair of the Italian Chapter of the IEEE RAS (2006-2010). He was awarded with the IEEE 2009 Chapter of the Year Award. He was a coeditor of two books by STAR, Springer Tracts in Advanced Robotics, Springer (2003 and 2005). His research interests include haptics, grasping, visual servoing, mobile robotics, and geometric control. He is an author of more than 200 papers in these fields. He is also a member of the IEEE.



Francesco Chinello received the MS degree in computer engineering from the University of Siena, Italy, in 2010. He is currently working toward the PhD degree in the Department of Information Engineering and Mathematics, University of Siena, and is a visiting student at the Department of Advanced Robotics of the Italian Institute of Technology. His research interests include developing and testing haptic and robotic systems, focusing on cutaneous force feedback for virtual interaction and teleoperation.



Claudio Pacchierotti (S'12) received the MS degree cum laude in computer engineering from the University of Siena, Italy, in 2011. He was an exchange student at the Karlstad University, Sweden, in 2010. He is currently working toward the PhD degree in the Department of Information Engineering and Mathematics, University of Siena, and in the Department of Advanced Robotics at the Italian Institute of Technology. His research interests include robotics and haptics, focusing on cutaneous force feedback techniques, wearable devices, and haptics in robotic surgery. He is a student member of the IEEE.



Monica Malvezzi (M'12) received the MS degree in mechanical engineering from the University of Florence in 1999, and the PhD degree in applied mechanics from the University of Bologna in 2003. She is an assistant professor of mechanics and mechanism theory at the Department of Information Engineering and Mathematics, University of Siena. Her primary research interests are in control of mechanical systems, robotics, vehicle localization, multibody dynamics, haptics, grasping, and dexterous manipulation. She is a member of the IEEE.

► For more information on this or any other computing topic, please visit our Digital Library at www.computer.org/publications/dlib.